Cell Reports, Volume *42*

Supplemental information

Microglia reactivity entails microtubule remodeling from acentrosomal to centrosomal arrays

Maria Rosito, Caterina Sanchini, Giorgio Gosti, Manuela Moreno, Simone De Panfilis, Maria Giubettini, Doriana Debellis, Federico Catalano, Giovanna Peruzzi, Roberto Marotta, Alessia Indrieri, Elvira De Leonibus, Maria Egle De Stefano, Davide Ragozzino, Giancarlo Ruocco, Silvia Di Angelantonio, and Francesca Bartolini

Supplementary Figures

SFigures

Figure S1. Analysis of EB and CAMSAP2 expression in homeostatic, activated and alternatively activated microglia. Related to Figure 3

Figure S2. Molecular, morphological and functional characterization of microglia non-centrosomal MTs nucleation in primary cultures and in retinal slices. Related to Figure 4

Figure S3. Analysis of pericentriolar material maturation during microglia activation. Related to Figure 5

Fig. S4. Inhibition of pericentriolar material maturation alters the number and size of blebbing extracellular vesicles. Related to Figure 5

Fig S5. Characterization of in vivo microglia activation in the LPS-induced uveitis model. Related to Figure 5

Fig.S1

A

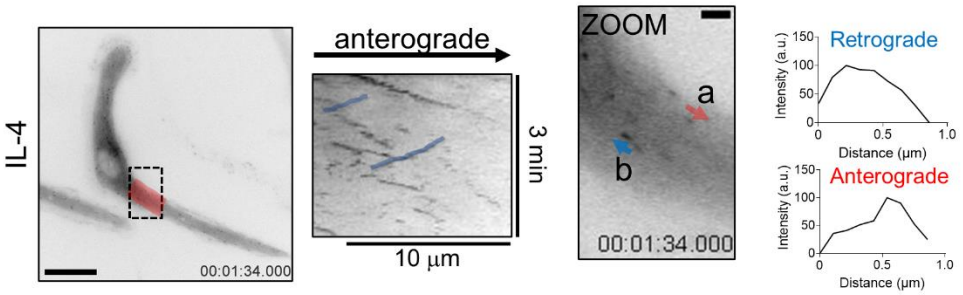

B

	Tyr⁺/EB⁺ comets	Tyr⁺/EB⁻ comets	TOT
Homeo	96	57	153
LPS-IFNγ	361	48	409
IL-4	146	33	179
TOT	603	138	741

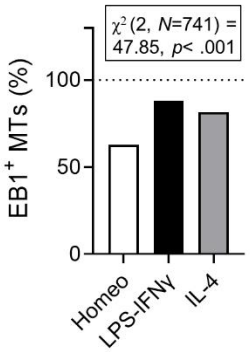

C

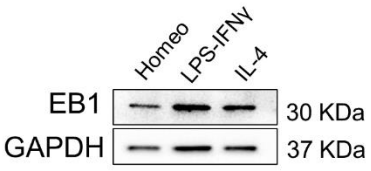

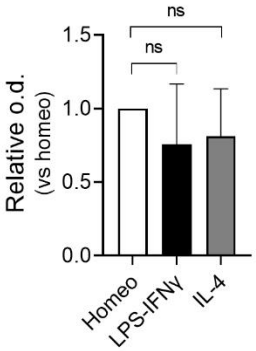

D

	Retrograde comets	Anterograde comets	TOT
Homeo	33	108	141
LPS-IFNγ	1	187	188
IL-4	32	224	256
TOT	66	519	585

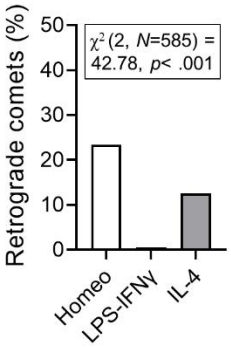

E

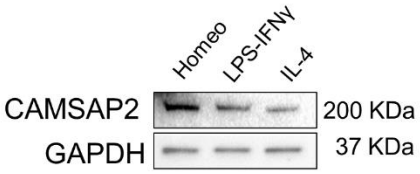

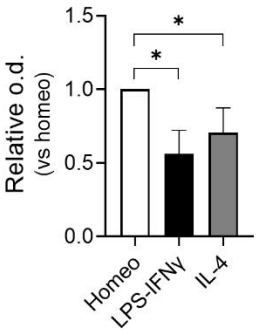

Fig. S1. Analysis of EB and CAMSAP2 expression in homeostatic, activated and alternatively activated microglia. Related to Figure 3

(A) *Left*, representative inverted contrast widefield frame from time lapse acquisitions of EB3-EGFP infected alternatively activated (IL-4) microglia (scale bar: 20 μm) and kymograph of the selected region in red (middle). Note that retrograde comets in the kymograph are highlighted in blue. *Right*, inverted contrast single frame image of EB3-EGFP at higher magnification (scale bar: 2 μm). Relative orientation of EB3 comet peaks with respect to the cell nucleus was used to distinguish between EB3 anterograde (a, red arrow) and retrograde (b, blue arrow) comets. **(B)** Contingency analysis of EB1 and tyrosinated α-tubulin (Tyr tub) co-staining in homeostatic (Homeo) condition and following LPS-IFNγ or IL4 treatment: percentage of double positive staining are reported in the bar chart, χ^2 parameters are reported in the insert. (**C**) *Bottom*: bar chart reporting the amount of EB1 protein level in microglia phenotypes; *top*: representative immunoblot of EB1. Values are expressed as median ± interquartile range from 4 independent experiments. p=0.31, Mann Whitney test. (**D**) Contingency analysis of comets in Homeo, LPS-IFNγ or IL-4 challenged microglia: percentage of retrograde comets are reported in the bar chart, χ^2 parameters are reported in the insert. (**E**) *Bottom*: bar chart reporting the amount of CAMSAP2 protein level in microglia phenotypes; *top*: representative immunoblot of CAMSAP2. Values are expressed as median ± interquartile range from 4 independent experiments. * $p < 0.05$, Mann Whitney test.

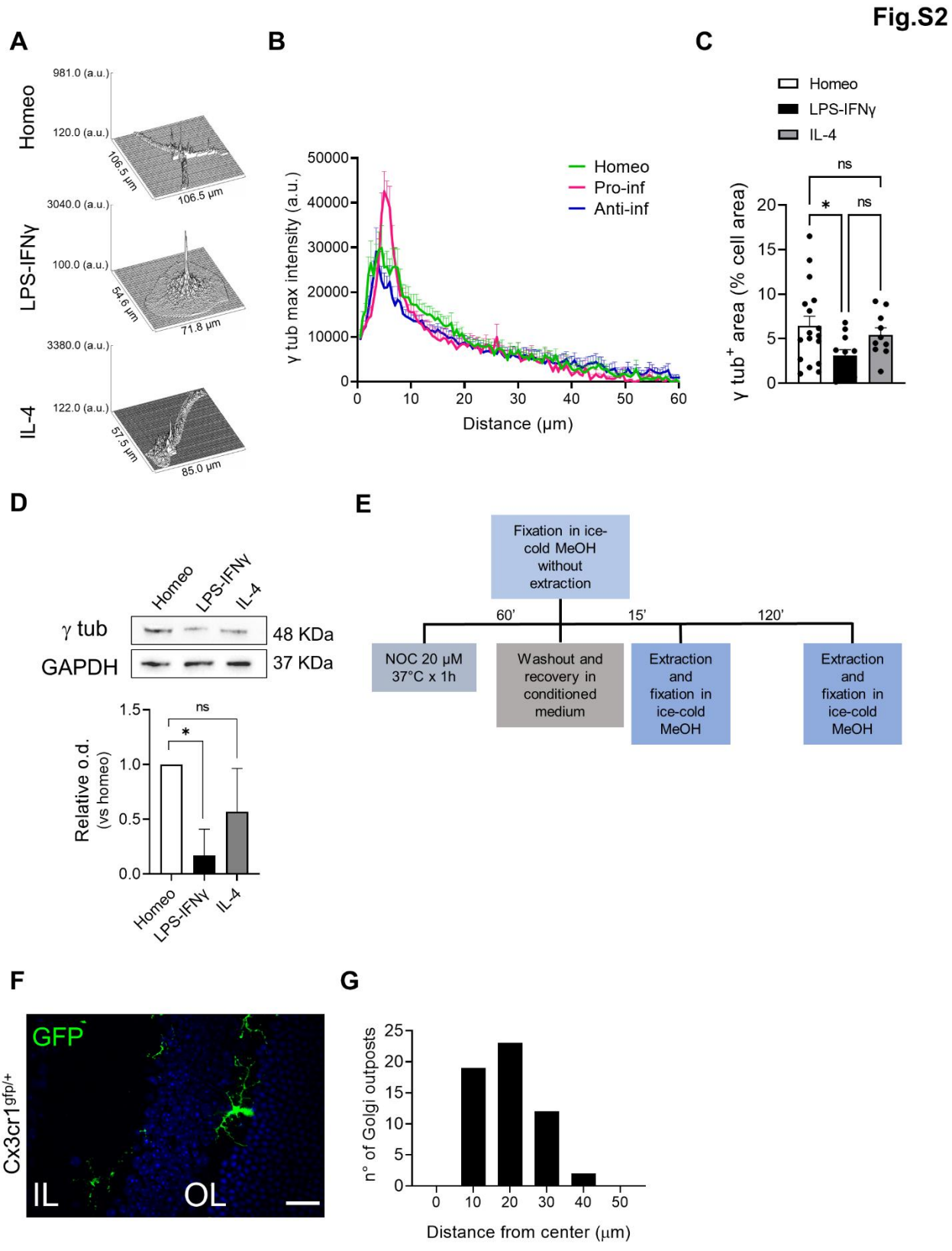

Fig. S2. Molecular, morphological and functional characterization of microglia non-centrosomal MTs nucleation in primary cultures and in retinal slices. Related to Figure 4

(A) Representative volumetric rendering of γ-tubulin (γ tub) signal intensity of homeostatic (Homeo) condition and following LPS-IFNγ or IL4 treatment. **(B)** Maximum fluorescence intensity values of γ tub vs the radial distance from the center of the nucleus, obtained with radial profiling in Homeo (n = 13 cells, green), LPS-IFNγ (n = 14 cells, magenta) and IL-4 (n = 14 cells, blue) challenged microglia. **(C)** Scatter dot plot showing analysis of γ tub signal over the cell area in Homeo, LPS-IFNγ and IL-4 conditions. Values are expressed as mean ± SEM (Homeo n = 17, LPS-IFNγ n = 11 and IL-4 n = 10 cells from 4 independent experiments). * $p < 0.05$, Kruskal-Wallis test - Dunn's multiple comparison test. **(D)** Representative immunoblot of total γ tub in Homeo, LPS-IFNγ and IL-4 treated microglia (*top*); bar chart showing the quantification of γ tub protein levels (*bottom*). Values are expressed as median ± interquartile range from 4 independent experiments. * $p < 0.05$, Mann Whitney test. **(E)** Treatment timeline of Nocodazole wash out assay. **(F)** Representative images of retinal slices (50 μm thickness) from control cx3cr1$^{gfp/+}$ mice stained with Hoechst for nuclei visualization (blue), showing retinal cell layers (IL inner layer, OL outer layer). Scale bar: 20 μm. **(G)** Bar chart reporting the number of Golgi outposts at increasing distance from the center of cell body in retinal microglia.

Fig.S3

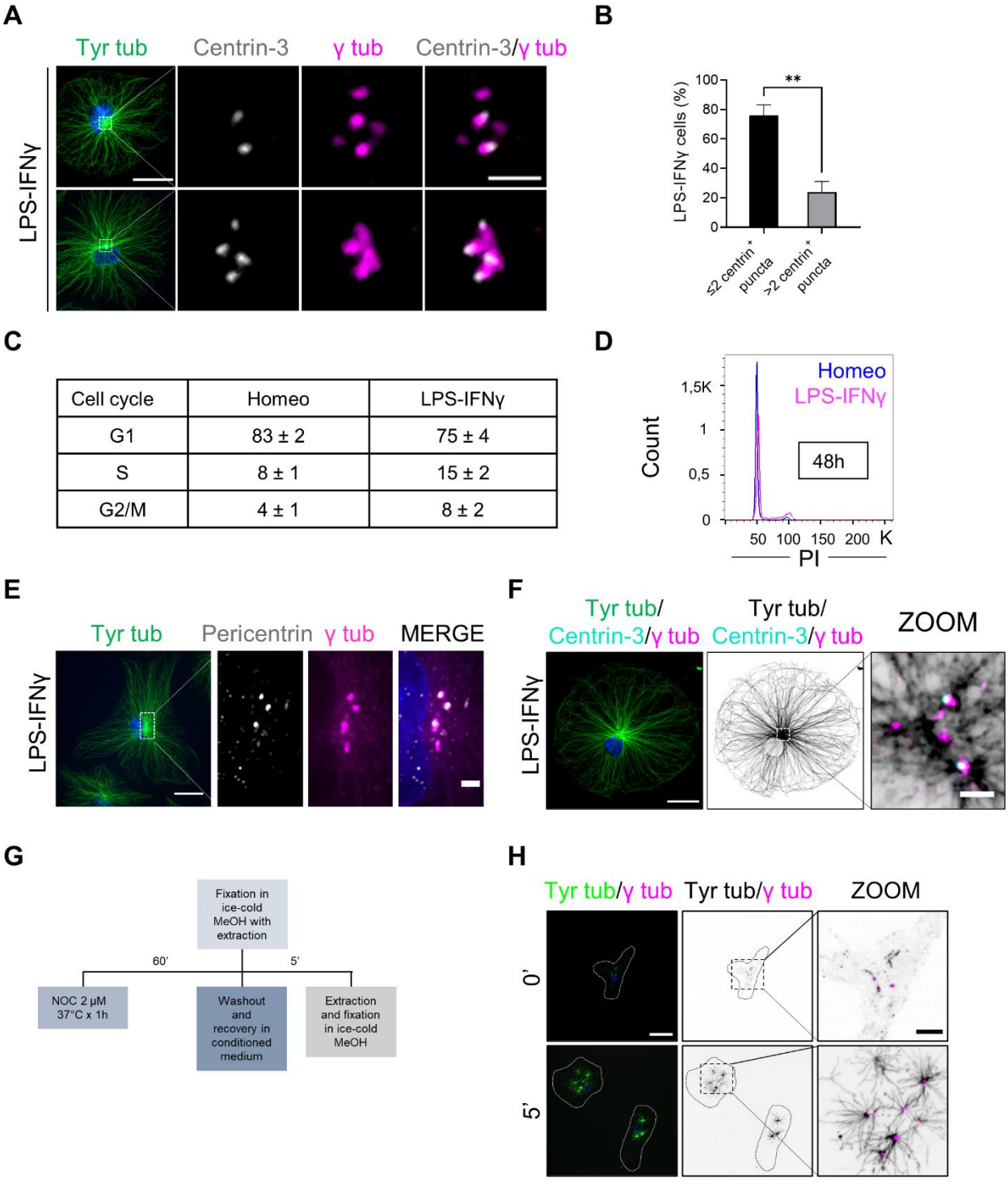

Fig. S3. Analysis of pericentriolar material maturation during microglia activation. Related to Figure 5

(A) Representative images showing tyrosinated α-tubulin (Tyr tub, green), centrin-3 (gray) and γ -tubulin (γ tub, magenta) immunolabeling and co-localization of centrin-3 (gray) and γ tub (magenta) in activated (LPS-IFNγ) microglia. Scale bar: 20 µm; zoom, 2 µm. Hoechst for nuclei visualization,

blue. **(B)** Bar graph reporting the percentage of LPS-IFNγ treated cells displaying ≤2 or >2 centrin^{+} puncta. Values are expressed as mean ± SEM of n = 52 cells from 3 independent experiments. **p <0.01, Student's t-test. **(C)** Table reporting the percentage of cells in G1, S and G2/M phases from Homeo and LPS-IFNγ treated microglia cultures, stained with propidium iodide (PI) and analyzed by flow cytometry. Percentages indicate the relative enrichment in cell population, values are expressed as mean ± SEM from three independent experiments. **(D)** Representative histogram of cell cycle overlay of Homeo (blue line) and LPS-IFNγ (magenta line) treated microglia. **(E)** Representative images showing Tyr tub (green), pericentrin (gray) and γ tub (magenta) immunolabeling in LPS-IFNγ treated microglia. Scale bar: 20 µm; zoom, 2 µm. Hoechst for nuclei visualization, blue. **(F)** *Left:* representative image of Tyr tub (green), centrin-3 (cyan) and γ tub (magenta) immunolabeling in LPS-IFNγ challenged microglia. *Middle* and *right:* representative image showing Tyr tub (black, inverted LUT), centrin-3 (cyan) and γ tub (magenta) immunolabeling in LPS-IFNγ treated microglia. Out of focus blur was removed using "remove haze" filter in Metamorph Software to highlight the asters. Scale bar: 20 µm; zoom, 2 µm. Hoechst for nuclei visualization, blue. (**G)** Treatment timeline of Nocodazole wash out assay of LPS-IFNγ challenged microglia. **(H)** Representative confocal images of the time course of the MT re-nucleation assay after nocodazole washout in LPS-IFNγ challenged microglia stained for Tyr tub (green) and γ tub (magenta). Scale bar: 20 µm; zoom: 5 µm. Hoechst for nuclei visualization, blue. Time 0' represents the MT depolymerizing effect of nocodazole in LPS-IFNγ treated cells with free tubulin extraction.

Fig.S4

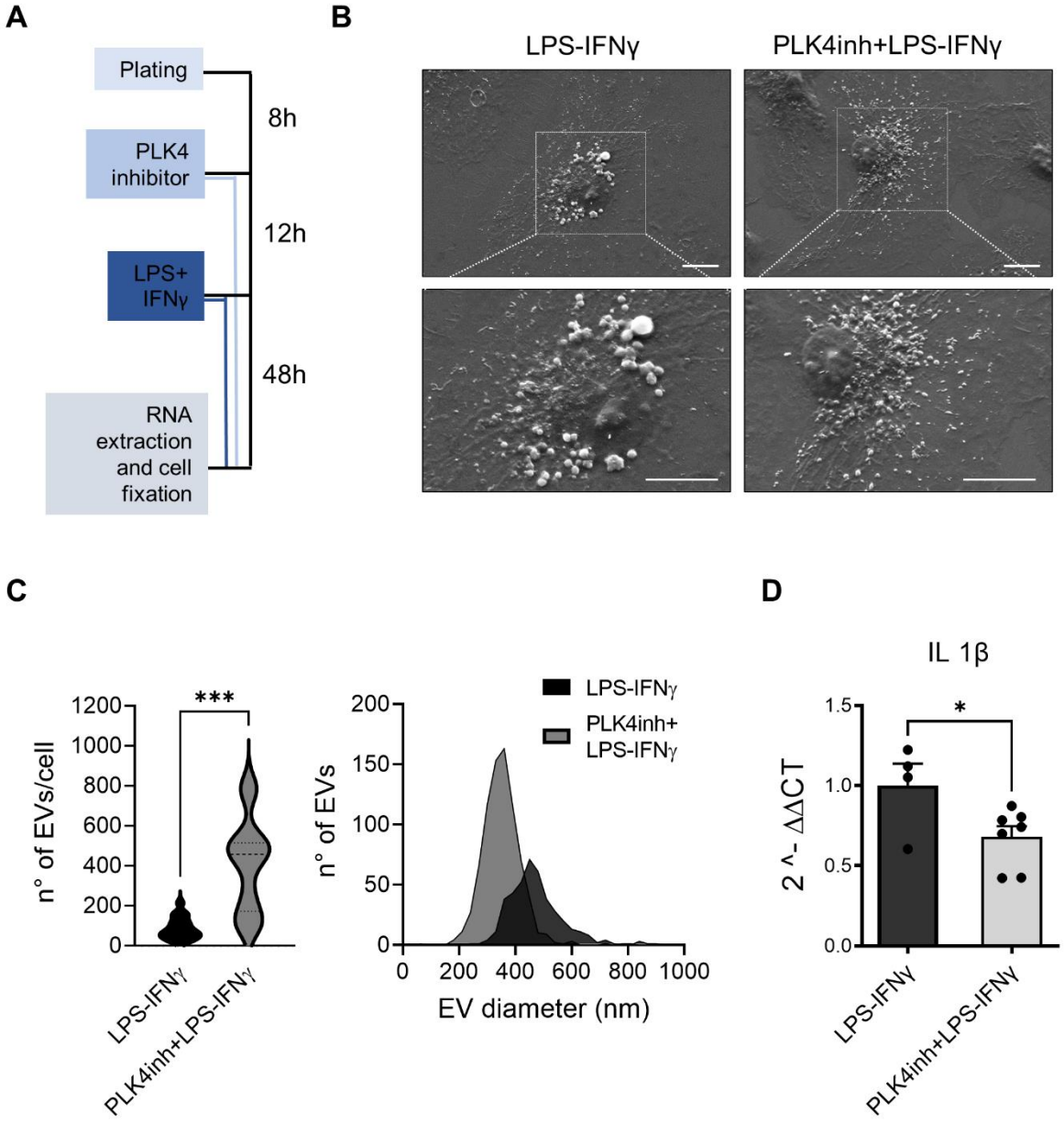

Fig. S4 Inhibition of pericentriolar material maturation alters the number and size of blebbing extracellular vesicles and Il-1β gene expression. Related to Figure 5

(A) Experimental timeline of PLK4 inhibitor treatment and pro-inflammatory cytokine administration. **(B)** Scanning electron micrographs showing extracellular vesicles (EVs) on the surface of LPS-IFNγ (*left*) and PLK4 inhibitor+LPS-IFNγ (*right*) treated microglia. Scale bar: 10 μm. **(C)** *Left*: violin plot showing the number of EVs in LPS-IFNγ challenged microglia with or without PLK4inh treatment (LPS-IFNγ n = 17 cells, PLK4 inhibitor+LPS-IFNγ n = 19 cells from 2 independent cultures; *** p <0.001, Student's t-test). *Bottom*: distribution of EV size measured on cell surface of LPS-IFNγ and PLK4 inhibitor+LPS-IFNγ treated microglia (LPS-IFNγ n = 17 cells, PLK4 inhibitor+LPS-IFNγ n = 19 cells). **(D)** Scatter dot plot reporting Il-1β gene expression upon

LPS-IFNγ or PLK4 inhibitor+LPS-IFNγ treatment, as revealed by RT-qPCR. Gene expression was normalized to the housekeeping gene *Gapdh*, n = 4 independent cultures. * p <0.05, Student's t-test.

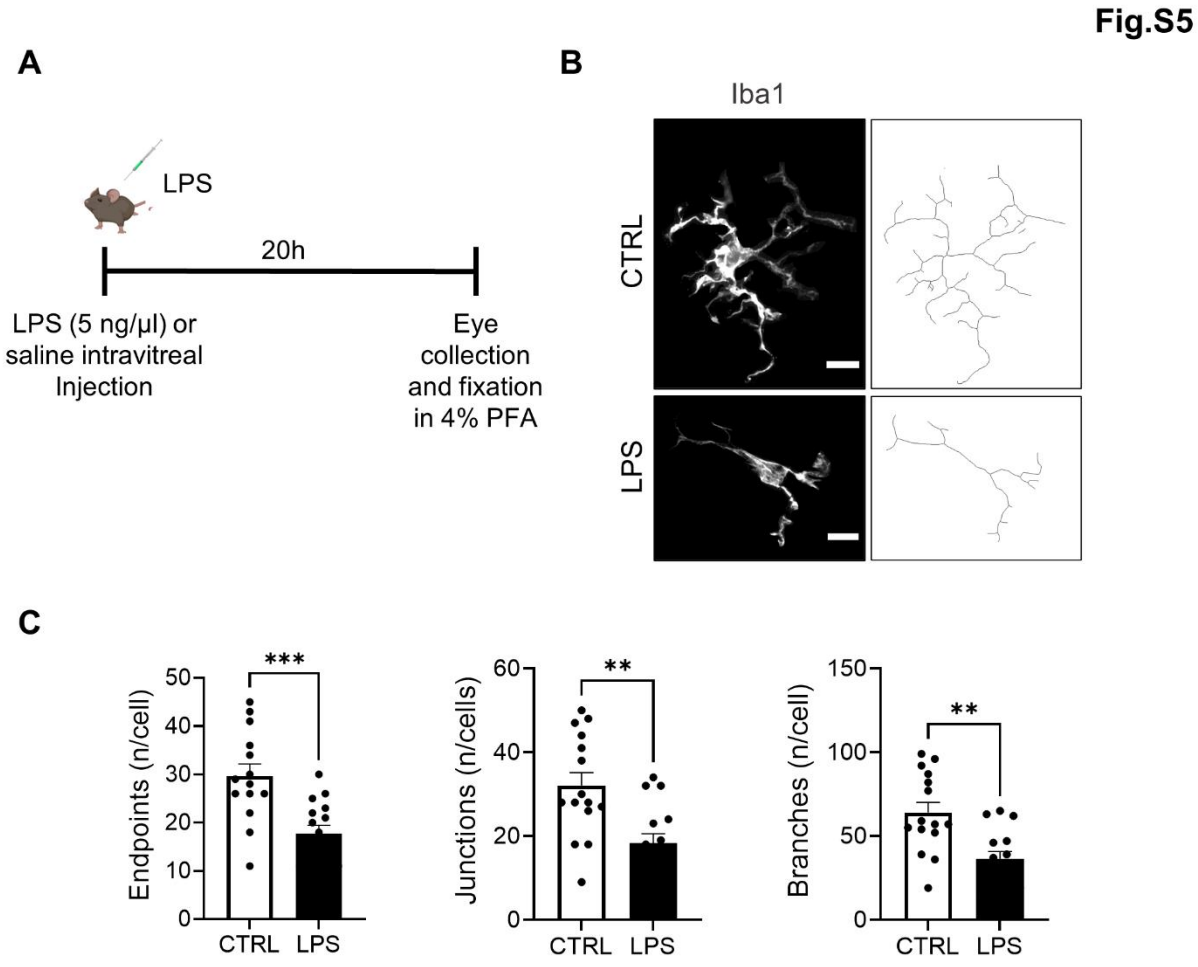

Fig. S5. Characterization of *in vivo* microglia activation in the LPS-induced uveitis model. Related to Figure 5

(A) Schematic illustration of surgical procedure and tissue collection. **(B)** *Left*: representative immunofluorescence images of microglia (Iba1, gray) in retinal slices (50 µm thickness) from CTRL (sham) and LPS treated mice. Scale bar: 10 µm. *Right*: corresponding skeletonized images. **(C)** Scatter dot plots reporting microglia arborization parameters as endpoints (*left*), junctions (*middle*) and branches (*right*) obtained from skeleton analysis of retinal microglia from CTRL (sham) and LPS treated mice. Values are expressed as mean ± SEM (CTRL, n = 14/3 cells/mice; LPS, n = 15/3 cells/mice; *** p <0.001, ** p <0.01; Student's t-test.